



Thermally induced transition from a ferromagnetic to a paramagnetic state in nanocrystalline FeAl processed by high-pressure torsion

C. Mangler^{a,*}, C. Gammer^a, K. Hiebl^b, H.P. Karnthaler^a, C. Rentenberger^a

^a University of Vienna, Faculty of Physics, Physics of Nanostructured Materials, Boltzmannngasse 5, 1090 Vienna, Austria

^b University of Vienna, Department of Physical Chemistry, Waehringner Strasse 42, 1090 Vienna, Austria

ARTICLE INFO

Article history:

Received 27 July 2010

Received in revised form 2 December 2010

Accepted 3 December 2010

Available online 15 December 2010

Keywords:

Ferromagnetism

High pressure torsion

Vacancies

Anti-phase boundary tubes

Nanocrystalline FeAl

Magnetic transition

ABSTRACT

The B2 ordered intermetallic compound FeAl shows a paramagnetic to ferromagnetic transition upon plastic deformation. The magnetic transformation is caused by the formation of a high density of antiphase boundary (APB) tubes leading to an increased number of Fe–Fe nearest neighbour pairs. In the present study it is shown that the temperature of the back transition from the ferromagnetic to the paramagnetic state depends strongly on the deformation mode. FeAl deformed by high pressure torsion (HPT) is investigated by differential scanning calorimetry, transmission electron microscopy and magnetic measurements. Based on the results of FeAl made nanocrystalline and disordered by HPT, it is concluded that the state of ferromagnetism vanishes almost completely at temperatures before re-ordering of the B2 long-range order has been encountered. This is in contrast to the findings reported for ball-milled FeAl indicating that the magnetic back transition and re-ordering occur at the same temperature. A model based on a vacancy driven change of Fe–Fe nearest neighbour configurations is proposed to explain the magnetic back transition after HPT deformation occurring at much lower temperatures.

© 2011 Published by Elsevier B.V.

1. Introduction

The intermetallic compound FeAl is paramagnetic in its B2 phase; it shows a transformation to a ferromagnetic state upon deformation or ion irradiation [1,2]. Several publications are dealing with this matter including various deformation methods like cold rolling, ball milling or nanoindentation [3–5]. The origin of the magnetic transition is attributed to disordering by the formation of anti-phase boundaries leading to an increased number of Fe–Fe nearest neighbour pairs, that are responsible for ferromagnetism [6]. The ferromagnetic state is a metastable one and vanishes upon heating, when the ordered B2 phase is restored. This was investigated by differential scanning calorimetry (DSC) studies combined with magnetic measurements [4].

In the present work, B2 ordered FeAl is deformed by high pressure torsion (HPT) leading to a disordered nanocrystalline structure that is ferromagnetic in agreement with the results in the literature. However, striking differences arise when the evolution of the ferromagnetic state upon heating is studied: ferromagnetism disappears at a temperature that is well below the temperature of re-ordering or dislocation recovery.

2. Experimental procedure

Fe–45 at.% Al specimens made from high purity Fe (99.99%) and Al (99.9997%) were annealed at 400 °C for one week. This treatment was used to achieve a defined initial state of order and vacancy concentration [7]. Samples (8 mm in diameter, 0.8 mm thick) were deformed by HPT up to 3 rotations under a pressure of 8 GPa to achieve deformation grades larger than 10,000%. The deformation was done at room temperature that corresponds to a temperature of 0.18 T_m (melting temperature). For DSC and transmission electron microscopy (TEM) investigations discs of 2.3 mm diameter were prepared from the outer rim of the HPT samples. For magnetic measurements samples of the same region were used.

Magnetic measurements of the as-deformed state were carried out using a SUS-10 magnetometer; the samples were in situ heated to 180 °C at a rate of 10 K/min at an applied field of 0.1 T.

DSC studies of the nanocrystalline samples were carried out using a Netsch DSC 204 Phoenix device in aluminium crucibles under argon flux at a heating rate of 10 K/min. Each sample was subjected to two subsequent heating runs and the second one was used as baseline.

For the TEM studies deformed samples were heated in the DSC to 130 and 170 °C followed by immediate cooling. Subsequently, TEM foils were prepared by twin-jet electropolishing in a solution of methanol with 33% nitric acid at –25 °C [8]. The TEM investigation of the different samples were carried out at RT using a Phillips CM200 operating at an acceleration voltage of 200 kV. The analysis of the electron diffraction patterns was done using the PASAD tools [9].

3. Experimental results

Fig. 1a shows a TEM bright-field image of the as-deformed state revealing a high density of defects in the grains and irregular, fragmented grain boundaries. In samples heated to 130 and 170 °C no

* Corresponding author.

E-mail address: clemens.mangler@univie.ac.at (C. Mangler).

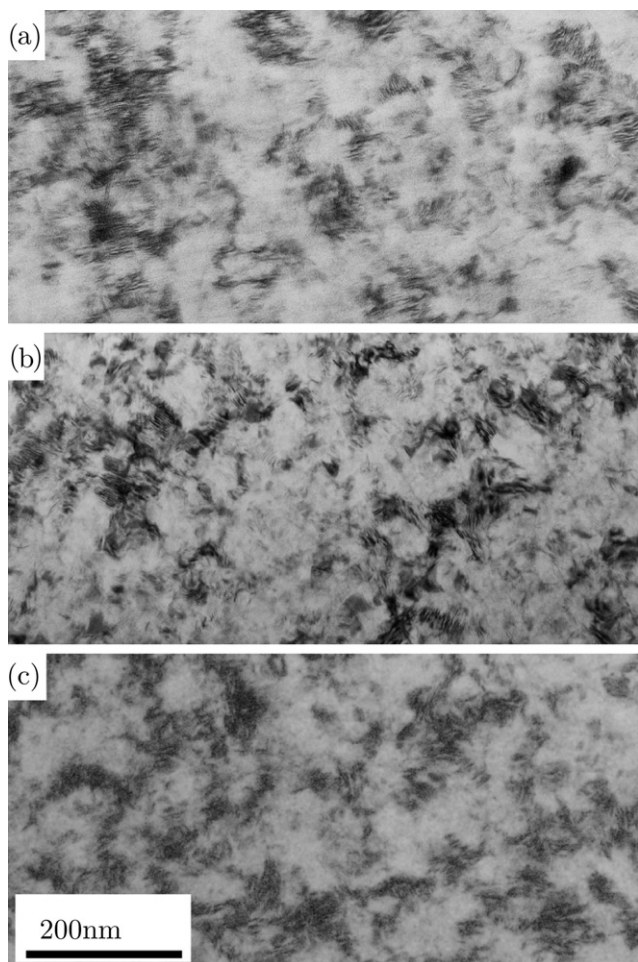


Fig. 1. TEM bright-field images of HPT deformed FeAl; (a) as deformed, (b) after heating up to 130 °C and (c) after heating up to 170 °C. No visible structural changes are encountered after heating.

visible structural change is observed compared to the as-deformed state (cf. Fig. 1b and c).

To study the evolution of the B2 long-range order by heating, electron diffraction studies were carried out. Fig. 2 shows the intensity profiles obtained by azimuthal integration of TEM selected area

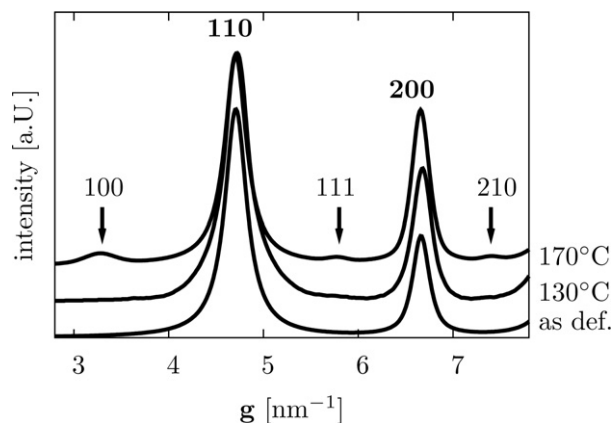


Fig. 2. HPT deformed FeAl, intensity profiles (intensity versus diffraction vector g) obtained by azimuthal integration of TEM diffraction patterns taken from the as-deformed state and from samples heated to 130 and 170 °C. While the fundamental reflections ((1 1 0), (2 0 0)) are present in all profiles, superlattice reflections (indicated by arrows) are clearly present at 170 °C showing, that re-ordering takes place at temperatures above 130 °C.

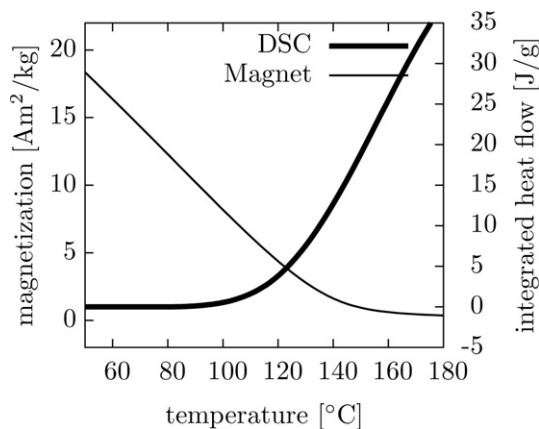


Fig. 3. Magnetisation and integrated heat flow (DSC signal) as measured by heating up of HPT deformed FeAl. At temperatures below 130 °C nearly no exothermic signal is measured. However, the deformation induced ferromagnetism decreases rapidly and vanishes above 130 °C.

diffraction patterns obtained from the as-deformed state and the samples heated to 130 and 170 °C. While the deformed sample and the sample heated to 130 °C show similar profiles, the profile obtained from the sample heated to 170 °C shows clear indications of reflections corresponding to the B2 superstructure (1 0 0, 1 1 1, 2 1 0).

The results of the magnetic studies carried out during in situ heating are shown in Fig. 3. The magnetisation that was induced by deformation decreases rapidly upon heating and vanishes at about 140 °C. In contrast, the integrated heat flow obtained during the DSC measurements shows no change below 120 °C, while above 120 °C a large heat flow is measured indicating the occurrence of exothermic processes.

4. Discussion

It is generally accepted that deformation induced ferromagnetism of non-magnetic intermetallics can be attributed to the formation of nearest neighbour Fe–Fe pairs. This can be achieved by deformation induced APB faults forming APB tubes [3,10,11]. In highly deformed specimens their density can be very high since they do not give rise to long range stresses like dislocations. APB tubes have been observed and analysed in intermetallic compounds e.g., in L_{12} [12–15] and B2 [16,17]. Due to the processes of their formation in B2, APB tubes consist of APB faults on {1 1 0} planes as shown in Fig. 4. During further deformation, the intersection of glide dislocations (consisting of two superpartial dislocations bounding an APB fault) with an APB tube leads to the formation of APB faults containing a step. A sketch of an interacting dislocation with a planar APB fault is given in Fig. 5. Consequently, the high dislocation activity during severe plastic deformation increases the area of APB faults and leads to a high density of stepped APB tubes. Fe atoms at the edges of the steps contribute to the occurrence of ferromagnetism; they have 3 Fe atoms in nearest neighbour posi-

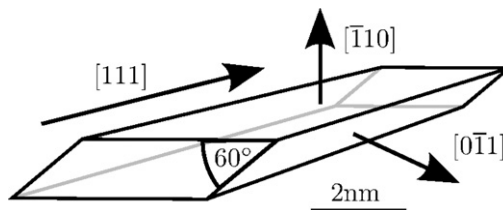


Fig. 4. Sketch of an antiphase boundary tube in B2 ordered FeAl composed of two sets of {1 1 0} planes and lying along the [1 1 1] direction.

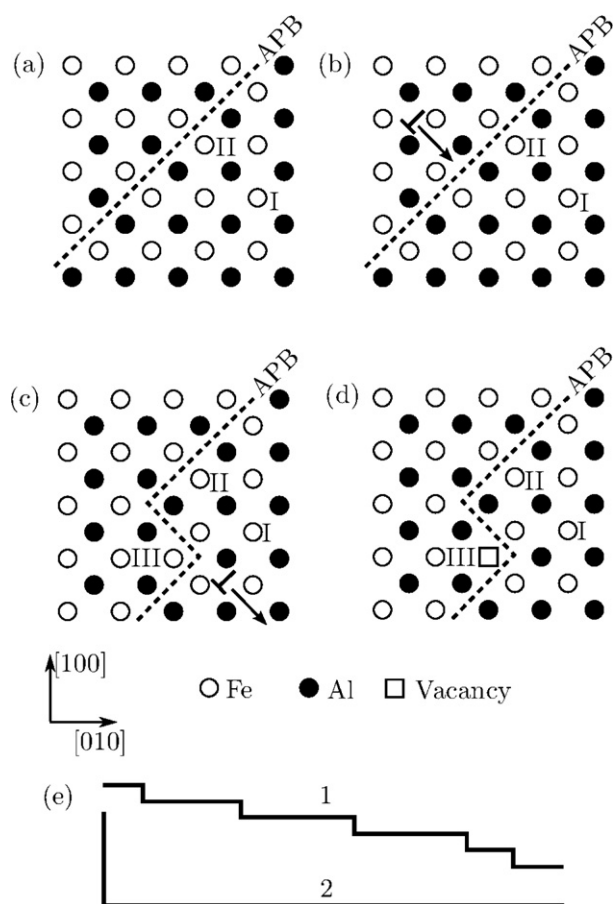


Fig. 5. (a–c) Schematic drawing of the intersection of a dislocation with an antiphase boundary tube in B2 ordered FeAl; projection along $[001]$. A planar APB fault (a) intersected by a superlattice dislocation (b) shows a step parallel to the $\{110\}$ glide plane of the moving dislocation (c). Three types of Fe-sites are formed yielding different configurations of nearest neighbours: in the ordered volume (I), at an APB (II) and at the edge of an APB (III). The number of the nearest neighbours as well as the resulting magnetic moments corresponding to the sites are listed in Table 1. (d) A vacancy at the edge of an APB step (III) reduces the Fe–Fe nearest neighbours. (e) APB before (1) and after (2) migration of vacancies along APB faults. The area of the APB fault is not altered, while the number of edges is reduced.

tions (cf. site III in Fig. 5 and Table 1), which is sufficient according to the local environment model to cause ferromagnetism [6]. One has to point out, that the schematics in Fig. 5 and Table 1 assume ideal stoichiometric composition. In the iron rich regime the excess Fe atoms are placed on Al sites; the fraction of such antisites increases with increasing Fe content and increases the saturation magnetisation [7].

While the magnitude of the ferromagnetism induced by HPT deformation is in good agreement with the results obtained by other deformation processes (e.g., cyclic deformation [11,18], ball milling [19–21] or cold rolling [3]) the present results obtained by in situ heating are different. Studies on the thermal evolution of the ferromagnetism induced by deformation processes like cold

Table 1

Magnetic moment and number of Fe–Fe nearest neighbours at different Fe sites: in the B2 ordered volume (I), at an APB (II) and at the edge of an APB (III). Only Fe atoms at the sites III are relevant for the ferromagnetism [6]. The sites I, II and III are shown in Fig. 5.

Fe site	Number of Fe–Fe nearest neighbours	Magnetic moment
I	0	$0 \mu_B$
II	2	$0 \mu_B$
III	3	$0.7 \mu_B$

rolling or ball milling show a direct correlation of the loss of ferromagnetism with the restoration of the LRO [3,4]. This is expected, since re-ordering is achieved by recovery of APB faults. The present results obtained from HPT deformed FeAl however show the disappearance of the ferromagnetic state at temperatures below 130°C . In this temperature regime no re-ordering processes leading to an exothermic signal in the DSC curve have been encountered (cf. Fig. 3) which is clearly confirmed by the diffraction data (cf. Fig. 2). Re-ordering by the growth of ordered domains as deduced from TEM studies [22] starts at temperatures $>130^\circ\text{C}$ where ferromagnetism has already vanished.

Therefore, we propose a vacancy based model for the disappearance of the ferromagnetic state: the HPT process induces a very high vacancy concentration due to the very high hydrostatic pressure [23]. Since disordering is accompanied with lattice expansion [4,24] it is assumed that vacancies will interact with APB faults representing disordered planes. Comparing migration enthalpies of the vacancies in disordered and long-range ordered FeAl (1.1 eV and 1.7 eV, respectively [25]) it is safe to assume that at low temperatures vacancy-related processes will take place at the APB faults. By vacancy jumps to the Fe-sites at the edges of the APB tubes (cf. site III in Fig. 5) the number of Fe–Fe nearest neighbours is lowered below 3 causing the transition to a paramagnetic state (cf. Table 1). Furthermore, the motion of vacancies along APB faults can lead to an accumulation of the steps and therefore to a reduction of edges (cf. state (1) and (2) in Fig. 5). These processes do not lead to a change in the overall APB area and are therefore not revealed in the DSC signal. Therefore, migration of vacancies and the reduction of the density of edges could lead to the disappearance of ferromagnetism. Finally, the difference of the present result to that of ball-milled samples could be explained by (i) an increase of the iron content during milling, (ii) by contamination and (iii) a reduced vacancy density. The first two points are mentioned in the literature showing an increase of the transition temperature with iron content and contamination by ball milling [19]. The third point, the reduced vacancy density in ball milled samples could be caused by the cyclic short time heating occurring during ball milling.

5. Conclusions

The loss of deformation induced ferromagnetism in high pressure torsion deformed FeAl occurs at temperatures that are well below those at which re-ordering is measured by DSC and TEM PASAD methods. This result is in contradiction to the findings reported for the deformation of ball milling. To explain the present result a model is proposed based on the large vacancy concentration that is present in HPT deformed samples. Two processes are considered: (i) the reduction of the density of Fe–Fe nearest neighbour sites by the reduction of steps in the antiphase boundaries by vacancy motion and (ii) the occupation of Fe–Fe nearest neighbour sites by vacancies.

Acknowledgments

The authors thank Prof. H. Sassik (TU Wien, Vienna, Austria) for help with preparation of the initial alloy, Prof. R. Pippan (ESI, Leoben, Austria) for support during the HPT deformation and the Austrian Science Fund (FWF):[P22440]. C.M. acknowledges support by the Austrian Science Fund (FWF):[S10403]. C.G. acknowledges the support by the IC “Experimental Materials Science – Nanostructured Materials”, a college for PhD students at the University of Vienna. Furthermore, the authors acknowledge the research project “Bulk Nanostructured Materials” within the research focus “Materials Science” of the University of Vienna.

References

- [1] R. Bernal-Correa, A. Rosales-Rivera, P. Pineda-Gómez, N.A. Salazar, *Journal of Alloys and Compounds* 495 (2) (2010) 491–494, doi:10.1016/j.jallcom.2009.08.085.
- [2] E. Menendez, M.O. Liedke, J. Fassbender, T. Gemming, A. Weber, L.J. Heyderman, K.V. Rao, S.C. Deevi, S. Surinach, M. Dolores Baro, J. Sort, J. Nogues, *Small* 5 (2) (2009) 229–234, doi:10.1002/sml.200800783.
- [3] Y. Yang, I. Baker, P. Martin, *Philosophical Magazine B* 79 (1999) 449–461.
- [4] S. Gialanella, X. Amils, M.D. Baro, P. Delcroix, G.L. Caer, L. Lutterotti, S. Surinach, *Acta Materialia* 46 (1998) 3305–3316.
- [5] J. Sort, A. Concustell, E. Menendez, S. Surinach, K.V. Rao, S.C. Deevi, M.D. Baro, J. Nogues, *Advanced Materials* 18 (13) (2006) 1717, doi:10.1002/adma.200600260.
- [6] H. Okamoto, P.A. Beck, *Monatshefte für Chemie* 103 (3) (1972) 907–921, doi:10.1007/bf00905453.
- [7] H. Xiao, I. Baker, *Acta Metallurgica et Materialia* 43 (1995) 391–396.
- [8] K. Yoshimi, M.H. Yoo, S. Hanada, *Acta Materialia* 46 (1998) 5769–5776.
- [9] C. Gammer, C. Mangler, C. Rentenberger, H.P. Karnthaler, *Scripta Materialia* 63 (2010) 312–315, doi:10.1016/j.scriptamat.2010.04.019.
- [10] D Wu, P.R. Munroe, I. Baker, *Philosophical Magazine* 83 (3) (2003) 295–313.
- [11] K. Yamamoto, S. Miyazaki, S. Kumai, A. Sato, *Philosophical Magazine* 83 (2003) 1431–1449.
- [12] C. Rentenberger, T. Waitz, H.P. Karnthaler, *Physical Review B – Condensed Matter and Materials Physics* 67 (9) (2003) 941091–941095.
- [13] C. Rentenberger, C. Mangler, H.P. Karnthaler, R. Pippan, S. Scheriau, *Materials Science Forum* 548–586 (2008) 422–427.
- [14] C. Rentenberger, C. Mangler, H.P. Karnthaler, *Materials Science and Engineering A* 387–389 (2004) 795–798.
- [15] D. Geist, C. Gammer, C. Mangler, C. Rentenberger, H.P. Karnthaler, *Philosophical Magazine* 90 (35–36) (2010) 4635–4645, doi:10.1080/14786435.2010.482178.
- [16] C.T. Chou, P.M. Hazzledine, P.B. Hirsch, G.R. Anstis, *Philosophical Magazine A: Physics of Condensed Matter, Structure, Defects and Mechanical Properties* 56 (6) (1987) 799–813.
- [17] K. Yamashita, M. Imai, M. Matsuno, A. Sato, *Philosophical Magazine A: Physics of Condensed Matter, Structure, Defects and Mechanical Properties* 78 (1998) 285–303.
- [18] H.Y. Yasuda, R. Jimba, Y. Umakoshi, *Scripta Materialia* 48 (2003) 589–592.
- [19] Q. Zeng, I. Baker, *Intermetallics* 14 (2006) 396–405.
- [20] D. Negri, A.R. Yavari, A. Deriu, *Acta Materialia* 47 (1999) 4545–4554.
- [21] R.A. Varin, T. Czujko, J. Bystrzycki, A. Calka, *Materials Science and Engineering A* 329–331 (2002) 213–221.
- [22] C. Mangler, C. Gammer, H.P. Karnthaler, C. Rentenberger, *Acta Materialia* 58 (17) (2010) 5631–5638, doi:10.1016/j.actamat.2010.06.036.
- [23] E. Schafner, G. Steiner, E. Korznikova, M. Kerber, M.J. Zehetbauer, *Materials Science and Engineering: A* 410–411 (2005) 169–173.
- [24] A. Korner, H.P. Karnthaler, *Philosophical Magazine A: Physics of Condensed Matter, Structure, Defects and Mechanical Properties* 52 (1) (1985) 29–38.
- [25] K. Reimann, H.J. Fecht, H.E. Schaefer, *Scripta Materialia* 44 (8–9) (2001) 1999–2003.